PHYSICAL REVIEW B

Tunneling microscopy of 2H-MoS₂: A compound semiconductor surface

M. Weimer, J. Kramar, C. Bai, and J. D. Baldeschwieler California Institute of Technology, Pasadena, California 91125 (Received 8 September 1987; revised manuscript received 23 December 1987)

Molybdenum disulfide, a layered semiconductor, is an interesting material to study with the tunneling microscope because two structurally and electronically different atomic species may be probed at its surface. We report on a vacuum scanning tunneling microscopy study of 2H-MoS₂. Atomic resolution topographs and current images show the symmetry of the surface unit cell and clearly reveal two distinct atomic sites in agreement with the well-known x-ray crystal structure.

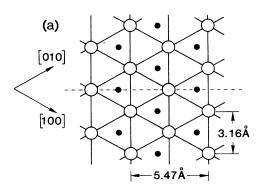
Over the last several years, scanning tunneling microscopy (STM) has emerged as a powerful tool for the realspace visualization of surface structures on an atomic scale. While the technique has enjoyed enormous success in elucidating several classical problems of geometric and electronic structure on homogeneous metallic and semiconducting surfaces, there remains a central problem with respect to the study of compound surfaces: to what extent can the chemical identity of individual atomic species be ascertained? Recently, progress in this area was made by Feenstra, Stroscio, Tersoff, and Fein² who succeeded in selectively imaging either Ga or As atoms in voltagedependent STM scans of GaAs(110), but so far this is the only case where such selectivity has been achieved. In an effort to add to our understanding of compound surface imaging by tunneling microscopy, we have undertaken a vacuum STM study of 2H-MoS₂, a layered semiconducting transition-metal dichalcogenide.

Layered compounds in general, and the transitionmetal dichalcogenides in particular, have played a prominent role in tunneling microscopy. Much of the emphasis has been on metallic members of this family, such as TaS₂ and TaSe2, where the surface charge rearrangement accompanying charge-density-wave formation has been observed in the low-temperature work of Coleman et al.³ The atomic corrugation of NbSe₂ has also been observed at room temperature, by Bando et al., who distinguished three different sites which they interpreted in terms of the two nonequivalent halves of the surface unit cell. ⁴ Those results, obtained at tunnel gap resistances of $3 \times 10^5 \Omega$, or less, showed unusually large corrugation amplitudes which the authors attributed to strong forces between the probe tip and sample surface. 5

Molybdenum disulfide is a new surface for STM studies. Since it is semiconducting, one expects its surface electronic wave functions to be preferentially localized over specific atoms or bonds. In this paper we show that it is possible to distinguish two distinct atomic sites at the surface of 2H-MoS₂ by tunneling microscopy, both in the conventional constant-current, variable-height mode of operation (without obtaining anomalously large corrugation amplitudes) as well as in the variable-current, constant-height mode.6

The crystal structure of molybdenum disulfide as determined by x-ray diffraction⁷ is shown in Fig. 1. From the point of view of the (001) surface projection, the top layer is a hexagonal lattice of sulfur atoms with lattice constant 3.16 Å. Immediately below this plane is an identical hexagonal lattice of molybdenum atoms laterally displaced relative to the top layer. The position of the Mo atoms reduces the sixfold S planar rotational symmetry to threefold symmetry, producing a diamond-shaped surface unit cell with a Mo atom centered in one triangular half and a hollow located in the other. Viewed from the side, one finds a repeated structure of two, alternating, S-Mo-S sandwiches separated by a van der Waals gap along which cleavage occurs.

MoS₂ in the 2H polytype is naturally occurring and mineralogical samples come in both n- and p-type with varying levels of doping. The highly anisotropic layer structure produces a substantial reduction in electrical conductivity perpendicular to the planes relative to that exhibited in plane. 8 Though we have not always found it necessary to do so, the data reported here were obtained



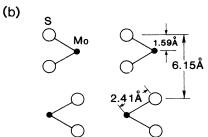


FIG. 1. (a) The (001) surface structure and (b) the (110) cross section [along the dashed line in (a)] of 2H-MoS₂, as determined by x-ray diffraction.

<u>37</u>

with crystals whose edges were coated with silver paint in order to take advantage of this higher in-plane conductivity. The doping level was not characterized, so the contribution of the sample spreading resistance to the total gap resistances we measure cannot be estimated.

The tunnel microscope used in these studies is patterned after the IBM Zurich "pocket-size" STM, ⁹ and is supported by a dual-stage spring suspension for additional vibration isolation. Scanning, data acquisition, and image display are all done under microcomputer control. After mounting and cleaving in air, our samples were pumped down to approximately 2×10^{-8} Torr without baking. All of the scans illustrated here were performed with an electrochemically etched W tip, but similar images have been obtained with other W tips and with electrochemically etched Au tips, on several different MoS₂ samples.

Figure 2 shows an atomic resolution constant-current topograph of the surface of 2H-MoS₂ obtained at positive sample bias so that electrons tunneled from the tip into unoccupied states of the sample. The image was acquired in 24 sec at a scan rate of 125 Å/sec and subsequently low-pass filtered. A centered hexagon of bright spots is evident in the figure, as are three distinct sites corresponding to the two constituent atom types and a surface hollow. An overlay of the surface unit cell is illustrated for comparison with Fig. 1. We see four bright spots at the corners, a secondary site in one half of the unit cell and a hollow in the other half, in agreement with the x-ray crystal structure.

Figure 3 displays the change in surface height along cross-sectional cuts indicated by the dashed lines in Fig. 2. Figure 3(a) shows the height versus distance along a [110] cell diagonal with a major peak, a secondary peak, and a hollow clearly visible. The peak-to-hollow corrugation amplitude is roughly 0.5 Å while the difference in height between the major and secondary peaks is approximately half as large. We note that the corrugation inferred from tunneling is much smaller than the 1.59 Å separating atomic centers in the top layer from those in the second. Figure 3(b) depicts the corrugation along a

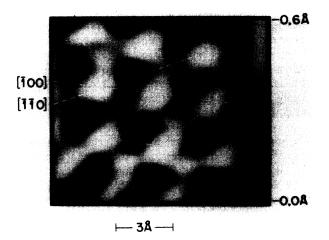


FIG. 2. Topographic image of the surface of $2H\text{-}MoS_2$ at +140 mV sample bias and 2-nA tunnel current. Grey scale indicates vertical range.

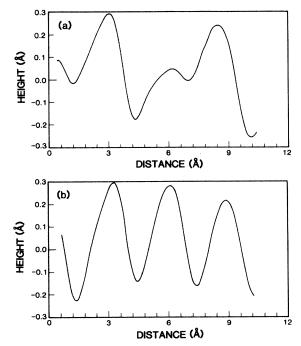


FIG. 3. Interpolated cross sections through the data of Fig. 2: (a) along the $[\bar{1}\ \bar{1}\ 0]$ cell diagonal and (b) the $[\bar{1}\ 0\ 0]$ cell edge.

 $[\bar{1}\,00]$ cell edge, where only a simple sinusoidal modulation is evident. The peak-to-hollow amplitude measured there is almost as large as that along the $[\bar{1}\,\bar{1}\,0]$ cell diagonal.

Figure 4 shows an atomic resolution current-contrast image of the same surface. Again, tunneling is into the sample. The image was acquired in 1.6 sec at a scan rate of 1350 Å/sec and then low-pass filtered. The vertical scale reflects the ac variation in tunnel current relative to

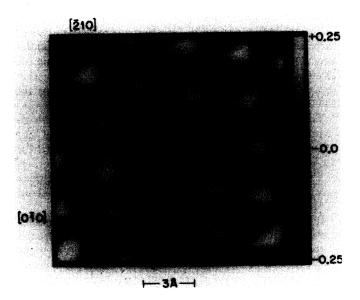
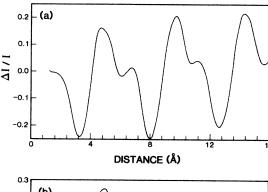


FIG. 4. Variable current image of the surface of 2H-MoS₂ at +250 mV sample bias and 2 nA mean tunnel current. Grey scale indicates ac current modulation relative to mean current.



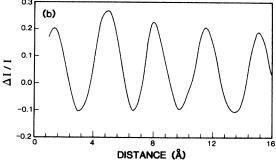


FIG. 5. Interpolated cross sections through the data of Fig. 4: (a) along the $[\bar{2}20]$ cell diagonal and (b) the $[0\bar{1}0]$ cell edge.

its mean value.

The centered hexagonal pattern of bright spots is especially vivid, and the definition in the three distinct sites superior to that of Fig. 2. This difference presumably arises from the greater external noise immunity associated with the fast scan mode⁶ and the complete absence of thermal drift. The bright spots and hollows appear roughly circular whereas threefold symmetry is apparent in the secondary sites. An overlay of the familiar surface unit cell shows the expected structure. When we plot the variation in tunnel current relative to its mean value along the directions indicated in Fig. 4 we find a repeated pattern of three sites along the cell diagonal, and sinusoidal modulation along the cell edge, as illustrated in Fig. 5. Along the [210] cell diagonal the total peak-to-hollow corrugation represents a variation of 50% in $\Delta I/I$ while along the [010] cell edge it is less, as required by symmetry.

The lateral distance scales in Figs. 3 and 5 are those inferred from the nominal expansion coefficients of our ceramics and none of the figures has been corrected for piezo nonorthogonality. As a result, the unit-cell overlays of Figs. 2 and 4 appear slightly distorted while the peak spacings and hollow locations in Fig. 5 all vary by about \pm 10% from the correct values indicated in Fig. 1.

It was our experience that we did not usually obtain such high-quality images of 2H-MoS₂ on initial approach of the tip to the sample, but had to spend some time scanning over the surface first. Images appeared more easily and consistently in the current-contrast mode than in the topographic mode, but atomic resolution was by no means automatic in either case. This may have been due in part

to our particular samples, which displayed a high degree of surface roughness relative to graphite, making the task of atomic resolution imaging more difficult. Qualitatively similar results were observed at negative sample bias.

We cannot rule out the possibility that a multiple-atom tip 10 is responsible for the structure we report on here, as a number of different images were observed as a function of time and presumably tip condition. Nevertheless, the Fourier transform of Fig. 4 produces the sixfold symmetric power spectral density expected for this surface. Information on the two sites per unit cell is contained in the relative phases associated with each of these six directions, reducing the apparent sixfold symmetry to the appropriate threefold one. The symmetry of the Fourier transform together with the accurate position of the second site within the unit cell requires a precise spatial phase relationship between hypothesized multiple tips. In our view, such an artifice is rendered less likely by the frequency with which this configuration is observed independent of probe-tip composition.

A more straightforward interpretation of our results directly identifies the two sites in these images with the two surface atomic species. Simple geometric considerations would then imply the brightest points are due to sulfur atoms, which are closest to the tip, while the secondary peaks arise from molybdenum atoms in the second layer. The predominant factor governing tunneling microscope images, however, is the contribution made by each atom's valence orbitals to the position- and energydependent density of states (near E_F) at distances above the surface normally associated with tunneling. 11 Numerous theoretical investigations of the band structure of 2H-MoS₂ (Ref. 12) point to strongly covalent bonding with a substantial Mo 4d contribution at the top of the valence band and bottom of the conduction band. Thus, one cannot a priori ignore the possibility that Mo 4d levels, rather than S 3p levels, are primarily responsible for the tunnel current.

In conclusion, it appears possible to clearly resolve two chemically and structurally distinct atomic sites in a layered compound by tunneling microscopy. Since there are no intrinsic surface states on 2H-MoS₂ (Ref. 13) one should be able to directly probe the differences between tunneling into the conduction band (as we have done here) or out of the valence band, as first suggested by Tersoff and Hamann¹¹ and realized in the experiments of Feenstra et al. ² It will be interesting to see whether such experiments, combined with appropriate calculations, can uniquely establish the position of the transition-metal atom in this and other layered semiconductors.

The authors are indebted to Ch. Gerber for guidance and to W. J. Kaiser for constant advice and encouragement. We have benefited from stimulating conversations with D. Denley, T. Coley, and W. A. Goddard III. This work was supported by the Office of Naval Research, under Contract No. N00014-86-K-0214, by the National Institutes of Health, under Contract No. RO1 GM37226-01, and by a gift from the Shell Companies Foundation.

- ¹G. Binnig and H. Rohrer, IBM J. Res. Dev. 30, 355 (1986).
- ²R. M. Feenstra, J. A. Stroscio, J. Tersoff, and A. P. Fein, Phys. Rev. Lett. 58, 1192 (1987).
- ³R. V. Coleman, W. W. McNairy, C. G. Slough, P. K. Hansma, and B. Drake, Surf. Sci. 181, 112 (1987); C. G. Slough, W. W. McNairy, R. V. Coleman, B. Drake, and P. K. Hansma, Phys. Rev. B 34, 994 (1986); R. V. Coleman, B. Drake, P. K. Hansma, and C. G. Slough, Phys. Rev. Lett. 55, 394 (1985).
- ⁴H. Bando, H. Tokumoto, W. Mizutani, K. Wantanabe, M. Okano, M. Ono, H. Murakami, S. Okayama, Y. Ono, S. Wakiyama, F. Sakai, K. Endo, and K. Kajimura, Jpn. J. Appl. Phys. 26, L41 (1987).
- ⁵J. M. Soler, A. M. Baro, N. Garcia, and H. Rohrer, Phys. Rev. Lett. 57, 444 (1986).
- ⁶A. Bryant, D. P. E. Smith, and C. F. Quate, Appl. Phys. Lett. **48**, 832 (1986).
- ⁷R. G. Dickinson and L. Pauling, J. Am. Chem. Soc. **45**, 1466 (1923).

- ⁸A. J. Grant, T. M. Griffiths, G. D. Pitt, and A. D. Yoffe, J. Phys. C 8, L17 (1975).
- ⁹Ch. Gerber, G. Binnig, H. Fuchs, O. Marti, and H. Rohrer, Rev. Sci. Instrum. 57, 221 (1986).
- ¹⁰H. A. Mizes, Sang-il Park, and W. A. Harrison, Phys. Rev. B 36, 4491 (1987).
- ¹¹J. Tersoff and D. R. Hamann, Phys. Rev. B 31, 805 (1985); Phys. Rev. Lett. 50, 1998 (1983).
- ¹²E. Doni and R. Girlanda, in *Electronic Structure and Electronic Transitions in Layered Materials*, edited by V. Grasso (Reidel, Dordrecht, 1986), p. 72; R. Coehoorn, C. Haas, J. Dijkstra, C. J. F. Flipse, R. A. deGroot, and A. Wold, Phys. Rev. B 35, 6195 (1987).
- ¹³A. Koma and K. Enari, in *Physics of Semiconductors—1978*, edited by B. L. H. Wilson, IOP Conference Series No. 43 (Institute of Physics, Bristol, 1979), p. 895.

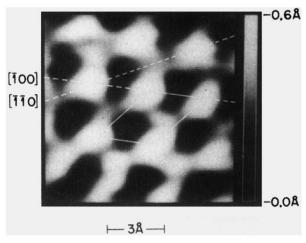


FIG. 2. Topographic image of the surface of $2H\text{-MoS}_2$ at +140 mV sample bias and 2-nA tunnel current. Grey scale indicates vertical range.

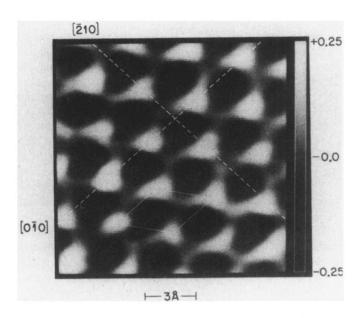


FIG. 4. Variable current image of the surface of 2H-MoS $_2$ at +250 mV sample bias and 2 nA mean tunnel current. Grey scale indicates ac current modulation relative to mean current.